JACS
JOURNAL OF THE AMERICAN CHEMICAL SOCIETY

Communication

pubs.acs.org/JACS

Bis(tridentate) Ruthenium–Terpyridine Complexes Featuring Microsecond Excited-State Lifetimes

Douglas G. Brown,[†] Nawaporn Sanguantrakun,[†] Benjamin Schulze,[‡] Ulrich S. Schubert,*[,‡] and Curtis P. Berlinguette*[,†]

[†]Department of Chemistry, Centre for Advanced Solar Materials, and Institute Sustainable Energy, Environment and Economy, University of Calgary, 2500 University Drive N.W., Calgary, Canada, T2N-1N4

[‡]Laboratory of Organic and Macromolecular Chemistry (IOMC) and Jena Center for Soft Matter (JCSM), Friedrich-Schiller-University Jena, Humboldtstr. 10, 07743 Jena, Germany

Supporting Information

ABSTRACT: A series of heteroleptic bis(tridentate) ruthenium(II) complexes, each bearing a substituted 2,2′:6′,2″-terpyridine (terpy) ligand, is characterized by room temperature microsecond excited-state lifetimes. This observation is a consequence of the strongly σ-donating and weakly π-accepting tridentate carbene ligand, 2′,6′-bis(1-mesityl-3-methyl-1,2,3-triazol-4-yl-5-idene)-pyridine (**C^N^C**), adjacent to the terpy maintaining a large separation between the ligand field and metal-to-ligand charge transfer (MLCT) states while also preserving a large ^{3}MLCT energy. The observed lifetimes are the highest documented lifetimes for unimolecular ruthenium(II) complexes and are four orders in magnitude higher than that associated with $[Ru(terpy)_2]^{2+}$.

The viability of ruthenium(II) photosensitizers in a myriad of applications (e.g., photodynamic therapy, molecular electronics, sensitization of semiconductors, artificial photosynthesis, environmental remediation) hinges on a high-energy excited state that is sufficiently long-lived to facilitate the desirable electron-/energy-transfer process or photochemical reaction.[1−7] The coordination complex, $[Ru(bpy)_3]^{2+}$ (bpy = 2,2′-bipyridine), and derivatives thereof have demonstrated remarkable utility in this regard due to redox stability in both the ground and excited states, a broad and tunable metal-to-ligand charge-transfer (MLCT) band in the visible region and a reasonably long excited-state lifetime (τ = 860 ns for $[Ru(bpy)_3](PF_6)_2$ in deaerated MeCN) with high emission quantum yields (Φ = 0.062).[1] This dynamic photophysical behavior is manifest in the lowest-lying ^{3}MLCT excited states being energetically resolved from the deactivating triplet metal-centered (^{3}MC) excited states (Supporting Information (SI), Figure S1). The related bis(tridentate) complex, $[Ru(terpy)_2]^{2+}$ (terpy = 2,2′:6′,2″-terpyridine; Figure 1), benefits from many of the same properties; however, the acute bite angle of the tridentate ligand renders the radiationless deactivating ^{3}MC states thermally accessible thus compromising the excited-state lifetimes (e.g., τ = 0.25 ns for $[Ru(terpy)_2](PF_6)_2$).[2] This outcome is unfortunate because the inherent C_2 symmetry of $[Ru(terpy)_2]^{2+}$ provides many synthetic advantages in that it circumvents isomerization issues, and enables easy incorporation into supramolecular assemblies through facile substitution at the 4′ position of the terpy ligand to promote vectorial electron transfer in said assemblies.[2,8] These observations provide the imperative to design bis(tridentate) platforms with longer excited-state lifetimes to, for example, render long-lived charge-separated states that can rival the photosynthetic construct.

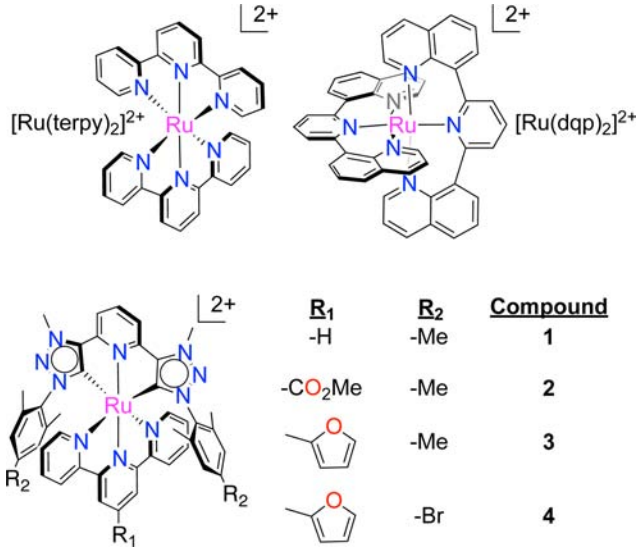

Figure 1. Benchmark and title ruthenium(II) complexes. (Counterion = BF_4^- for title complexes.)

One proven strategy to prolong excited-state lifetimes for bis(tridentate) ruthenium(II) complexes is to bestow a more idealized octahedral ligand environment[9−11] on the metal to increase the ligand field splitting and thus the energy difference between the ^{3}MLCT and ^{3}MC states. Hammarström et al. demonstrated the viability of this approach by showing that $[Ru(dqp)_2]^{2+}$ (dqp = 2,6-di(8′-quinolinyl)pyridine; Figure 1), where the metal exists in a nearly ideal octahedral environment, exhibits an excited-state lifetime of 3.0 μs.[12] It has since been inferred that symmetry reasons and, consequently, the extended shape of the ^{3}MLCT potential energy surface rather than ^{3}MC destabilization contributes to the long lifetime.[13] Although the

Received: April 24, 2012
Published: July 18, 2012

   dx.doi.org/10.1021/ja3039536 | J. Am. Chem. Soc. 2012, 134, 12354−12357

Table 1. Photophysical and Electrochemical Data for 1−4 and $[Ru(terpy)_2](PF_6)_2$

	1	2	3	4	$[Ru(terpy)_2](PF_6)_2$
λ_{abs} (nm)[a,b]	463 (1.0)	472 (1.0)	472 (1.0)	473 (1.0)	474 (1.8)[h]
λ_{em} (nm)[c]	643	688	691	694	–
τ (ns)[c]	385	1720	6980	7900	0.25[i]
Φ (%)[d]	11.4	7.5	2.5	1.7	
$E_{1/2,ox}$ (V)[e,f]	1.24	1.31	1.18	1.22	1.52[h]
$E_{1/2,red}$ (V)[e,f]	−1.31	−1.08	−1.33	−1.24	−1.02[h]
E_{0-0} (eV)[g]	2.09	2.02	2.02	1.98	2.13[h]

[a]Measured in MeCN at 298 K. Absorption maximum of lowest energy, spin-allowed MLCT band. [b]ε indicated in parentheses in units of $\times 10^4$ M^{-1} cm^{-1}. [c]Emission maximum generated by excitation at ∼470 nm; measured in deareated EtOH/MeOH (80:20, v/v). [d]Determined using $[Ru(bpy)_3](PF_6)_2$ as a standard. [e]Measured in MeCN using a 0.1 M NBu_4BF_4 supporting electrolyte and $[Fc]^+/[Fc]^0$ as a standard. [f]Reported vs NHE. [g]Determined by the intersection point of the absorption and emission curve, where the latter is normalized to the lowest energy ^{1}MLCT band. [h]Reported in ref 25. [i]Reported in ref 1.

5.5 μs lifetime of a derivative of this complex represents the longest reported room temperature lifetime for a ^{3}MLCT state in the literature to date for mononuclear ruthenium complexes,[14] this type of bis(tridentate) Ru(II) complex suffers from the formation of *mer* and *fac* isomers, while substitution of one dqp ligand with a terpy ligand significantly diminishes the lifetime of the complex to 7.4 ns.[12] An alternative strategy is to increase the energy gap between the ^{3}MC and ^{3}MLCT states by placing π acceptors on the polypyridyl ligand or to install anionic, σ- and π-donating auxiliary ligands (e.g., pbpy = 6-phenyl-2,2′-bipyridine).[5,15−21] While the latter approach often leads to lower lifetimes by virtue of the energy gap law (e.g., τ = 10 ns for $[Ru(terpy)(pbpy)]^{1+}$),[16,22,23] the work of Chung et al. demonstrated that the combination of the strong σ-donating and π-accepting character of charge-neutral *N*-heterocyclic carbene ligands can raise the energy of the ^{3}MC state while almost maintaining the ^{3}MLCT energy to render long-lived excited states.[24]

The separation between the ^{3}MC and ^{3}MLCT states can be further improved by utilizing even stronger σ-donating ligands as well as auxiliary substituents. Indeed, it was recently demonstrated in one of our laboratories[25] that ruthenium(II) complexes bearing mesoionic carbene ligands, such as 2′,6′-bis(1-mesityl-3-methyl-1,2,3-triazol-4-yl-5-idene)pyridine tetrafluoroborate (**C^N^C**), can render a long-lived excited-state lifetime (e.g., 633 ns for **1**;[25] Figure 1). We rationalized that further fine-tuning of the separation of the ^{3}MC and ^{3}MLCT states could be achieved by adding electron-withdrawing groups (EWGs) or electron-donating groups (EDGs) to the ligand scaffold to induce even longer lifetimes. Following this line of inquiry, we demonstrate herein that judicious installation of EWGs and EDGs about both tridentate ligands affords an electronic structure that leads to the longest room-temperature ^{3}MLCT lifetime ever reported for a complex bearing a single ruthenium center.

The title complexes were produced by the sequential coordination of the two tridentate ligands to the metal ion (synthetic details are provided as SI). Compounds **2**−**4** were synthesized in a similar manner to that of **1**[25] using mild and selective transmetalation reactions between silver-activated forms of the carbene ligands [namely, silver(I) complexes of **C^N^C** and 2′,6′-bis(1-(2,6-dimethyl-4-bromophenyl)-3-methyl-1,2,3-triazol-4-yl-5-idene)pyridine (**C^N^C-Br**)] and *cis*-[Ru(terpy-R_1)(DMSO)Cl_2] (R_1 = −H, 2-furyl, $-CO_2Me$ positioned at the 4′-position of terpy) derivatives (Scheme S1, SI). Notably, the *trans*-[Ru(terpy-R_1)(DMSO)Cl_2] derivatives were inert to reactions with said carbene precursors. The identity and purity of the dark-red microcrystalline solids were verified by ^{1}H and ^{13}C NMR spectroscopic techniques, elemental analyses, and matrix-assisted laser desorption/ionization (MALDI) and high-resolution electrospray-ionization (HR-ESI) mass spectrometry (see SI).

The electrochemical behavior of **1**−**4** in MeCN was examined by cyclic voltammetry (Table 1). Each complex exhibits a single reversible metal-based oxidation wave at ca. 1.2 V (all potentials reported herein are vs NHE). The Ru(III)/Ru(II) redox couple for **1** was measured to be 1.24 V, while the $-CO_2Me$ and −2-furyl groups positioned on the terpy ligands of **2** and **3** shift the HOMO energies to 1.31 and 1.18 V, respectively. Replacement of a methyl group belonging to each mesityl moiety of **3** with a bromo substituent (i.e., **4**) leads to a diminution of electron density on the metal thus lowering the HOMO energy to 1.22 V. Note that the halide is moderately σ-accepting and π-donating, but the latter is suppressed by the orthogonality of the mesityl and carbene groups of the **C^N^C** ligand.[26]

The trends in the first reductive waves for **1**−**4** indicate that the π^* systems of the terpy and **C^N^C** ligands of **1** are very close in energy.[25] The presence of the π acceptor on the terpy ligand lowers the LUMO, which is reflected by a ligand-based reduction potential for **2** that is 140 mV lower than that of **1** (Figure 2). The presence of the electron-donating 2-furyl group about the terpy in **3**, however, produces a ligand-based reduction potential at ca. 0.84 V that is consonant with **1**. This observation suggests that the π^* system of the terpy ligand is higher in energy and that the LUMO resides on the carbene ligand in **3** and **4**. This arrangement of energy levels is

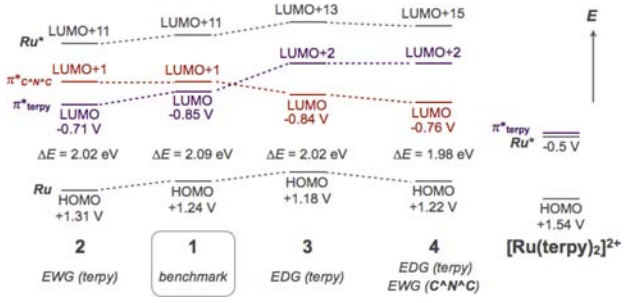

Figure 2. Summary of relevant energy levels for **1**−**4**. The HOMO and LUMO energies correspond to the ground- and excited-state oxidation potentials, respectively; the LUMO+1 and higher levels are estimated from computational data. Data for $[Ru(terpy)_2]^{2+}$ is also provided for comparison.

dx.doi.org/10.1021/ja3039536 | J. Am. Chem. Soc. 2012, 134, 12354−12357

supported by the disparities of the first reduction waves for **3** and **4**; i.e. a lower LUMO energy for **4**, where the carbene ligand features an additional acceptor (Figure 2).

The UV−vis absorption spectra of solutions of **2**−**4** (Figure 3) each reveal MLCT bands centered at ca. 470 nm with

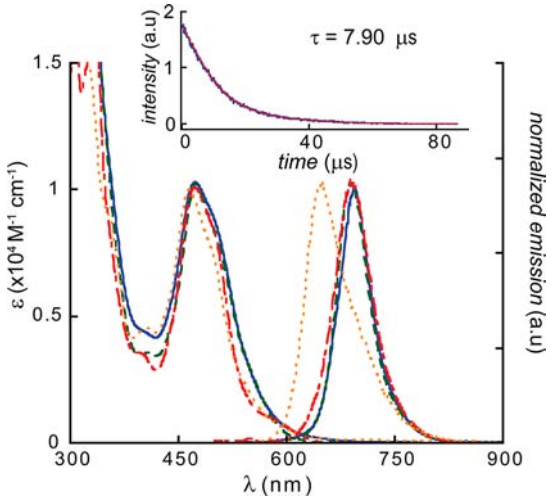

Figure 3. UV−vis absorption and emission spectra for **1** (orange), **2** (red), **3** (green), and **4** (blue) recorded in ethanol/methanol (80:20 v/v) at room temperature. Inset: Representative time-correlated single photon emission decay profile for **4** (blue) in deaerated ethanol/methanol (80:20 v/v) overlaid with a monoexponential fit (red).

moderate extinction coefficients (e.g., ∼1.0 × 10^4 M^{-1} cm^{-1}). The narrow MLCT band in the visible region for each complex is a manifestation of the C_{2v} symmetry and the nearly degenerate π^* orbitals of both ligands. Time-dependent DFT calculations were carried out with MeCN included in the model (IEFPCM-B3LYP/LanL2DZ) to aid the assignment of the spin-allowed absorption transitions (all molecular orbital representations were provided by DFT calculations; B3LYP/LanL2DZ). While the simulated MLCT bands are slightly blue-shifted relative to the measured spectra, there is reasonable agreement between the computational and experimental data (e.g., Figure 4). It was determined that the HOMO, HOMO-1, and HOMO-2 levels of **4**, for example, contain significant metal character (which is corroborated by the electrochemistry experiments) with some delocalization over the tridentate ligands. The low-lying unoccupied orbitals are localized primarily to the π^* networks of both ligands with the LUMO assigned to the **C^N^C-Br** ligand (Figure 4). The low-energy shoulder of the MLCT band appears to involve the π^* of the terpy ligand (λ_1), while the λ_2 transition, which is characterized by the highest oscillator strength of the transitions in the visible region, involves the promotion of an electron to the LUMO. The low-energy tail that extends beyond 600 nm is tentatively assigned as a spin-allowed HOMO−LUMO transition, but we cannot exclude the direct population of the ^{3}MLCT manifold. The transitions at λ < 400 nm correspond to a combination of MLCT and ligand-centered transitions (Figure S4, SI).

The orbitals for **1**−**3** are reasonably similar to that of **4** in that the HOMO-2 to HOMO levels are primarily metal-based and the low-lying unoccupied orbitals are confined to the π^* system of the two ligands. The computational data indicate that the LUMO shifts from the terpy ligand in **1** and **2** to the carbene in **3** and **4**. Thus, the excited-state electron density is expected to reside on the terpy for **2** but on the carbene ligand

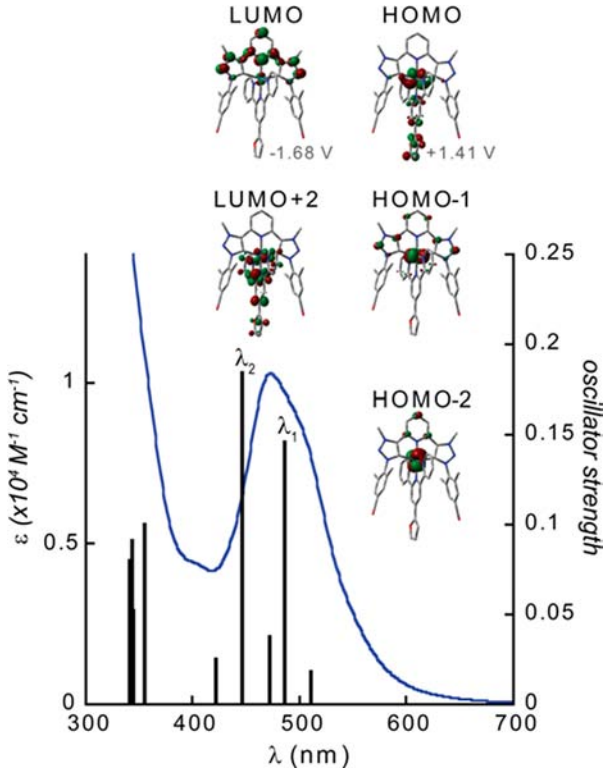

Figure 4. Experimental UV−vis absorption spectrum of **4** (blue trace) overlaid with calculated transitions represented by vertical bars. Details of the two largest calculated transitions (theoretical wavelength in nm, oscillator strength, % contribution to transition): λ_1: HOMO → LUMO+2 (486, 0.1464, 65%); λ_2: HOMO-2 → LUMO (446, 0.1848, 46%). Selected molecular orbitals are also shown; the calculated HOMO and LUMO levels are indicated.

for **3** and **4** in the ^{3}MLCT state.[27] Taking this feature into account along with the optical and electrochemical data, the relative energy levels appear to follow the order depicted in Figure 2. The presence of EWGs on the terpy, for example, lower the terpy-based LUMO to a greater extent than the metal-based HOMO, thereby inducing a bathochromic shift for **2** relative to **1**. The bathochromic shifts for **3** and **4** relative to **1** are consistent with the EDGs on the terpy inducing higher HOMO energies and a LUMO that is confined to the **C^N^C** ligands.

The emission spectra for **2**−**4** were measured in deaerated ethanol/methanol (80:20 v/v) solutions at 298 K upon excitation at wavelengths corresponding to the maximum of the MLCT band at ca. 470 nm. Each complex was characterized by a Stokes shift in excess of 200 nm, which is consistent with phosphorescence decay. Similar experiments performed in air revealed a partial quenching of the emission band that is consistent with a triplet emitting state, and thus we ascribe the decay for **2**−**4** as emission from a ^{3}MLCT state. The E_{0-0} values were assigned as the energies corresponding to the intersections of the absorption and emission spectra, where each emission band was normalized to the MLCT band at ca. 470 nm. The E_{0-0} values were determined to be ca. 2 eV for the series (Table 1), with the largest and smallest E_{0-0} values being measured for **1** and **4**, respectively.

The excited-state lifetimes for **2**−**4** in deaerated solvents were measured by time-correlated single-photon counting to be 1.7−7.9 μs. These values are striking in that they are several orders of magnitude longer than τ values typically observed for

dx.doi.org/10.1021/ja3039536 | J. Am. Chem. Soc. 2012, 134, 12354−12357

the vast majority of ruthenium(II) chromophores bearing a terpy ligand, even though the mesoionic carbene ligand imposes a more strained ligand environment around the metal center (∠N−Ru−N = 154.3°) than terpy (∠N−Ru−N = 158.4°).[25] Moreover, the lifetime of **4** exceeds the longest ^{3}MLCT lifetimes achieved so far by any mononuclear ruthenium(II) complex.[8−10,17,28] Interestingly, the data for **1**−**4** does not strictly conform to the energy gap law: The shortest τ value is observed in the case with the largest energy gap (i.e., **1**) while the longest τ was measured for **4**, which is characterized by the smallest E_{0-0}. We therefore surmise that the longer τ values of **2**−**4** relative to **1** are governed primarily by the increased separation between the emitting ^{3}MLCT state and the deactivating ^{3}MC state (Figure 2). Lending support to a thermally inaccessible ^{3}MC state is the lifetimes at 77 K for complexes **2**−**4** (13−18 μs; Table S1, SI) being similar to that exhibited by $[Ru(terpy)_2](PF_6)_2$ (11 μs) at 77 K. The conjugated substituents of the terpy ligand may also have an auxiliary role on the τ values (0.39, 1.72, and 6.98 μs where R_1 = −H, −CO_2Me, and −2-furyl, respectively), but the increase in the τ value with the terminal bromides present in **4** is indicative of inductive effects on the carbene ligand playing a significant role in the photophysics.

To the best of our knowledge, the lifetimes of **3** and **4** are among the highest for any monometallic ruthenium(II) complexes where emission originates from a ^{3}MLCT state. These long-lived excited states are manifest in the strongly σ-donating and π-accepting ability of the carbene ligand resolving the ^{3}MLCT and ^{3}MC states, while the presence of EWGs or EDGs about the ligands helps to further separate these states. These collective results demonstrate the enormous potential of using mesoionic carbene complexes to modify the photophysical properties of ruthenium(II) complexes. Investigations are underway to gain a better understanding of the photophysical properties of these complexes and to examine their potential in light harvesting applications.

■ ASSOCIATED CONTENT

Supporting Information

Full experimental details and TD-DFT data for **2**−**4**. This material is available free of charge via the Internet at http://pubs.acs.org.

■ AUTHOR INFORMATION

Corresponding Author

ulrich.schubert@uni-jena.de; cberling@ucalgary.ca

Notes

The authors declare no competing financial interest.

■ ACKNOWLEDGMENTS

C.P.B. is grateful for support from the Canadian Natural Science and Engineering Research Council, Canada Research Chairs, Canadian Foundation for Innovation, and Canada School of Energy and Environment. B.S. is grateful to the Fonds der Chemischen Industrie for a Ph.D. scholarship.

■ REFERENCES

(1) Campagna, S.; Puntoriero, F.; Nastasi, F.; Bergamini, G.; Balzani, V. *Top. Curr. Chem.* **2007**, *280*, 117.

(2) Hofmeier, H.; Schubert, U. S. *Chem. Soc. Rev.* **2004**, *33*, 373.

(3) Ardo, S.; Meyer, G. J. *Chem. Soc. Rev.* **2009**, *38*, 115.

(4) Alstrum-Acevedo, J. H.; Brennaman, M. K.; Meyer, T. J. *Inorg. Chem.* **2005**, *44*, 6802.

(5) Bomben, P. G.; Robson, K. C. D.; Berlinguette, C. P. *Coord. Chem. Rev.* **2012**, *256*, 1438.

(6) Tyson, D. S.; Luman, C. R.; Zhou, X.; Castellano, F. N. *Inorg. Chem.* **2001**, *40*, 4063.

(7) Damrauer, N. H.; Cerullo, G.; Yeh, A.; Boussie, T. R.; Shank, C. V.; McCusker, J. K. *Science* **1997**, *275*, 54.

(8) Baranoff, E.; Collin, J.-P.; Flamigni, L.; Sauvage, J.-P. *Chem. Soc. Rev.* **2004**, *33*, 147.

(9) Schramm, F.; Meded, V.; Fliegl, H.; Fink, K.; Fuhr, O.; Qu, Z.; Klopper, W.; Finn, S.; Keyes, T. E.; Ruben, M. *Inorg. Chem.* **2009**, *48*, 5677.

(10) Breivogel, A.; Förster, C.; Heinze, K. *Inorg. Chem.* **2010**, *49*, 7052.

(11) Hammarström, L.; Johansson, O. *Coord. Chem. Rev.* **2010**, *254*, 2546.

(12) Abrahamsson, M.; Jäger, M.; Osterman, T.; Eriksson, L.; Persson, P.; Becker, H.-C.; Johansson, O.; Hammarström, L. *J. Am. Chem. Soc.* **2006**, *128*, 12616.

(13) Österman, T.; Abrahamsson, M.; Becker, H.-C.; Hammarström, L.; Persson, P. *J. Phys. Chem. A* **2012**, *116*, 1041.

(14) Abrahamsson, M.; Jäger, M.; Kumar Rohan, J.; Osterman, T.; Persson, P.; Becker, H.-C.; Johansson, O.; Hammarström, L. *J. Am. Chem. Soc.* **2008**, *130*, 15533.

(15) Robson, K. C. D.; Koivisto, B. D.; Yella, A.; Sporinova, B.; Nazeeruddin, M. K.; Baumgartner, T.; Grätzel, M.; Berlinguette, C. P. *Inorg. Chem.* **2011**, *50*, 5494.

(16) Koivisto, B. D.; Robson, K. C. D.; Berlinguette, C. P. *Inorg. Chem.* **2009**, *48*, 9644.

(17) Schulze, B.; Escudero, D.; Friebe, C.; Siebert, R.; Görls, H.; Sinn, S.; Thomas, M.; Mai, S.; Popp, J.; Dietzek, B.; González, L.; Schubert, U. S. *Chem.—Eur. J.* **2012**, *18*, 3785.

(18) Medlycott, E. A.; Hanan, G. S. *Chem. Soc. Rev.* **2005**, *34*, 133.

(19) Collin, J. P.; Beley, M.; Sauvage, J. P.; Barigelletti, F. *Inorg. Chim. Acta* **1991**, *186*, 91.

(20) Djukic, J. P.; Sortais, J. B.; Barloy, L.; Pfeffer, M. *Eur. J. Inorg. Chem.* **2009**, 817.

(21) Chi, Y.; Chou, P.-T. *Chem. Soc. Rev.* **2007**, *36*, 1421.

(22) Constable, E. C.; Thompson, A.; Tocher, D. A.; Daniels, M. A. M. *New J. Chem.* **1992**, *16*, 855.

(23) Collin, J. P.; Kayhanian, R.; Sauvage, J. P.; Calogero, G.; Barigelletti, F.; DeCian, A.; Fischer, J. *Chem. Commun.* **1997**, 775.

(24) Son, S. U.; Park, K. H.; Lee, Y.-S.; Kim, B. Y.; Choi, C. H.; Lah, M. S.; Jang, Y. H.; Jang, D.-J.; Chung, Y. K. *Inorg. Chem.* **2004**, *43*, 6896.

(25) Schulze, B.; Escudero, D.; Friebe, C.; Siebert, R.; Görls, H.; Köhn, U.; Altuntas, E.; Baumgaertel, A.; Hager, M. D.; Winter, A.; Dietzek, B.; Popp, J.; González, L.; Schubert, U. S. *Chem.—Eur. J.* **2011**, *17*, 5494.

(26) Ung, G.; Bertrand, G. *Chem.—Eur. J.* **2011**, *17*, 8269.

(27) For the T_1-optimized geometry of **1**, the excited electron is located on the carbene (see ref 25); similar studies are underway for **2**−**4**.

(28) There are examples of mononuclear ruthenium complexes with slightly longer lifetimes where emission is primarily ligand-based, e.g.: Wang, X. Y.; Del Guerzo, A.; Baitalik, S.; Simon, G.; Shaw, G. B.; Chen, L. X.; Schmehl, R. *Photosynth. Res.* **2006**, *87*, 83.